JOURNAL OF MATERIALS SCIENCE 10 (1975) 1659–1664

Crack propagation and fracture in silicon carbide

A. G. EVANS
Science Center, Rockwell International, Thousand Oaks, California, USA

F. F. LANGE
Metallurgy and Metals Processing Department, Westinghouse Research Laboratories, Pittsburgh, Pennsylvania, USA

Fracture mechanics and strength studies performed on two silicon carbides – a hot-pressed material (with alumina) and a sintered material (with boron) – have shown that both materials exhibit slow crack growth at room temperature in water, but only the hot-pressed material exhibits significant high temperature slow crack growth (1000 to 1400° C). A good correlation of the observed fracture behaviour with the crack growth predicted from the fracture mechanics parameters shows that effective failure predictions for this material can be achieved using macro-fracture mechanics data.

1. Introduction

Silicon carbide is one of the materials with good potential for high temperature structural use [1], and a study of crack propagation at elevated temperatures is thus an important requirement for assessing its structural capabilities [2]. In this paper we perform a comprehensive crack growth characterization for two dense silicon carbides: a hot-pressed material with an Al_2O_3 additive*, and a sintered material with a B additive†.

The primary crack growth parameters can be fully assessed by performing two series of tests, as described in detail elsewhere [2]: fracture mechanics tests which yield the fundamental relation between the stress intensity factor, K_I, and the crack velocity, V, for macrocrack propagation; and fracture strength tests as a function of the applied stress rate, which yield crack growth parameters for the small flaws which pre-exist in the material. Both data are obtained in the present studies for silicon carbide hot-pressed with Al_2O_3; only K_I versus V data were obtained for the SiC sintered with B.

2. Experimental

2.1. Hot-pressed SiC

The critical stress intensity factor, K_{IC}, was determined between room temperature and 1500° C using the double torsion method [3] utilizing two different specimen dimensions: 0.3 x 2.5 x 7.5 cm and 0.07 x 1.5 x 3 cm. The double cantilever beam method [4] was also used to determine room temperature K_{IC} values using specimens with the smaller dimensions. Pre-cracks were generated in the larger specimens from machined notches by applying a pre-selected force to each specimen in the double torsion fixture (while immersed in water at room temperature) until pop-in occurred. Pre-cracks were generated in the smaller specimens by a wedging technique. Crack velocity data were obtained using the larger specimens, in the load relaxation or constant displacement rate test modes [5] at room temperature, and in the constant load or constant displacement rate mode at elevated temperature [5].

Strength data were obtained between room temperature and 1400° C in the four-point flexural testing mode (outer span 0.640 cm) with specimens of dimensions 0.3 cm x 0.61 cm x 3.2 cm. The tests were performed at three different displacement rates at several of the test temperatures. The stress rate was computed by determining the loading rate from the load–time data and the specimen dimensions [6]. The

* Supplied by Norton Company.
† Supplied by the General Electric Company.

surfaces of all the specimens were finished with a 320 grit diamond wheel and the two edges on the tensile surface were beveled with 320 grit SiC abrasive paper.

2.2. Sintered SiC

The K_{IC} and K_I versus V data for this material were obtained using the double-torsion method, and specimens with dimensions 0.2 cm x 2.5 cm x 5 cm.

3. Results

3.1. Fracture mechanics

The critical stress intensity factor, K_{IC}, data at temperatures up to 1500° C are shown in Fig. 1. For the hot-pressed material, K_{IC} is essentially temperature invariant up to 1000° C (median, 4.0 MN m$^{-3/2}$)*, but decreases at higher temperatures (to 2.0 MN m$^{-3/2}$ at 1500° C).

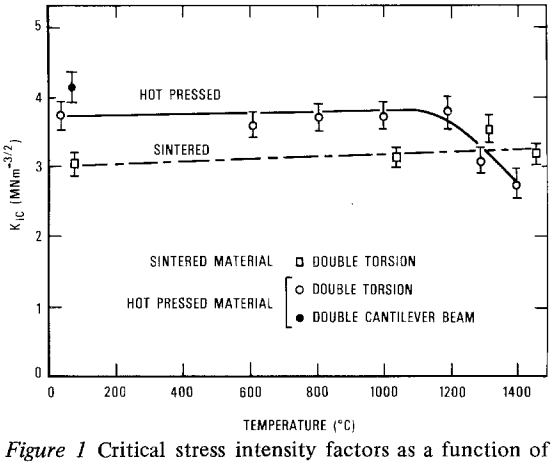

Figure 1 Critical stress intensity factors as a function of temperature for two silicon carbides.

For the sintered material, K_{IC} is temperature independent up to 1500° C, and has a median value of 3.0 MN m$^{-3/2}$. This material thus has a lower toughness than the hot-pressed material up to ~ 1350° C, but has a toughness advantage at higher temperatures.

Slow crack growth was detected in the hot-pressed material and has been extensively characterized at 25° C in water and at 600 and 1400° C in air (Fig. 2). The crack growth at each temperature can be described by the commonly used functional relation [2]:

$$V = AK_I^n \qquad (1)$$

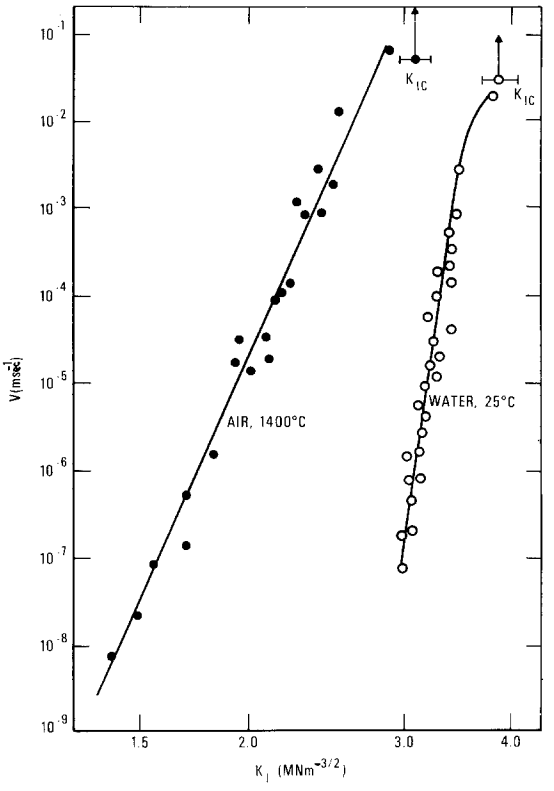

Figure 2 The stress intensity factor as a function of crack velocity for slow crack growth in the hot-pressed silicon carbide at room temperature in water and at 1400° C in air.

where A and n are constants for a given temperature and environment. At toom temperature the extent of the slow crack growth in water is minimal and n is a large number ~ 80. An apparent activation energy for slow crack growth, obtained using a differential temperature technique (see Appendix 1), is ~ 30 kcal mol^{-1}, similar to the values typically obtained for stress corrosion processes [7]. At 600° C, slow crack growth is hardly detectable ($n > 200$). At 1400° C extensive slow crack growth is apparent, $n \sim 21$, and the apparent activation energy for slow crack growth, ~ 120 kcal mol^{-1}, is in the range typically found for plastic flow related slow crack growth processes [5]. No significant gross deformation of the test specimens was detected in any of the tests, contrasting with the extensive deformation noted at low crack velocities in a hot-pressed silicon nitride at 1400° C [5].

A corresponding set of experiments for the sintered material did not detect any significant

* The reasonable correspondence of the double-torsion data (median, 3.9 MN m$^{-3/2}$), and the good agreement of the double torsion data independently obtained at two different laboratories using two different specimen sizes, add credence to the validity of the data.

slow crack growth at elevated temperatures (1000 to 1500° C); while in water at room temperature the slow crack growth was comparable in extent to that detected in the hot-pressed material (Fig. 2).

3.2. Strength tests

Four point flexural strength data for the hot-pressed material as a function of temperature, at a stress rate of $\sim 17\,\mathrm{MN\,m^{-2}\,sec^{-1}}$, are shown in Fig. 3. The strength decreases significantly with increase in temperature above $\sim 1000°$ C. Data obtained as a function of stress rate at 25, 1200, 1300 and 1400° C are shown in Fig. 4. These indicate an increase in strength with increase in stress rate at the elevated temperature, but no significant effect at the low temperature.

A small number of tests in argon and vacuum, at 1400° C and $\sim 17\,\mathrm{MN\,m^{-2}\,sec^{-1}}$, gave strength values (median, $320\,\mathrm{MN\,m^{-2}}$) similar to those in air (median $310\,\mathrm{MN\,m^{-2}}$) suggesting that there are no strong environmental effects on the crack propagation at this temperature.

4. Discussion

4.1. Crack growth analysis

The consistency of the fracture mechanics and strength data for the hot-pressed material can be assessed using an analysis which relates the fracture mechanics parameters to the stress-rate ($\dot{\sigma}$) dependence of the fracture stress, σ_f: notably [2, 8],

$$\sigma_f = \left[\frac{2\dot{\sigma}(n+1)}{AY^2(n-2)}\left(\frac{S}{K_{IC}}\right)^{n-2}\right]^{1/(n+1)} \qquad (2)$$

where S is the fracture stress (at the equivalent failure probability) in the absence of slow crack growth and Y is a geometric constant. Using the room temperature fracture stresses obtained in air (Fig. 3) as a measure of the fracture stress without slow crack growth, S, setting $Y = \sqrt{\pi}$, and introducing the fracture mechanics parameters, n and A, relations between σ_f and $\dot{\sigma}$ can be predicted for tests in water at room temperature and in air at 1400° C. The predicted strengths are compared with the measured strengths in Fig. 4. The correspondence is reasonable at room temperature* and excellent at 1400° C, establishing that the macro-fracture mechanics parameters, namely, K_{IC}, A and n, can be used to effectively predict the propagation of the small pre-existing flaws in this material.

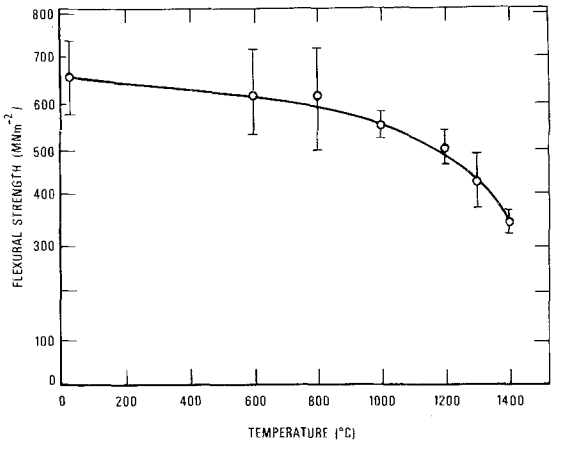

Figure 3 Four-point flexural strength data obtained for the hot-pressed silicon carbide as a function of temperature at a stress rate of $17\,\mathrm{MN\,m^{-2}\,sec^{-1}}$.

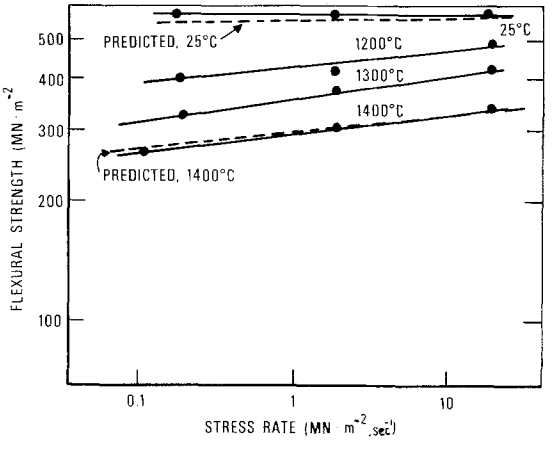

Figure 4 Flexural strength data as a function of stress rate for the hot-pressed silicon carbide at 25, 1200, 1300 and 1400° C. Also shown are the strengths at 25 and 1400° C predicted using both the fracture mechanics data (Fig. 2) and the 25° C strengths at $17\,\mathrm{MN\,m^{-2}\,sec^{-1}}$ (Fig. 3).

An apparent activation energy for slow crack growth obtained from the strength data (Appendix 1) is $130\,\mathrm{kcal\,mol^{-1}}$, which is consistent with the value obtained from the fracture mechanics tests ($120\,\mathrm{kcal\,mol^{-1}}$). This good correspondence further suggests that the direct application of fracture mechanics data is valid at least between 1200 and 1400° C.

* At room temperature, the predicted strengths lie within the scatter of the measured values, but they do not correspond to the mean values. This suggests that strength–stress rate measurements are not as sensitive as K_I versus V measurements in determining a materials susceptibility to sub-critical crack growth for large values of n.

Another verification of the utility of fracture mechanics data for predicting failure in hot-pressed SiC is given in Appendix 2.

4.2. Crack growth mechanisms at elevated temperatures for hot-pressed material

The absence of an environmental effect at high temperatures, combined with the relatively large apparent activation energy for slow crack growth is indicative of a plastic flow mechanism. Two primary sources of plastic flow induced slow crack growth have been postulated; a discrete dislocation process [9] and a grain-boundary sliding process [9, 10] (due to a viscous grain-boundary phase). The information generated in this study is not extensive enough to unambiguously distinguish between these possibilities, but by combining with complementary information obtained by Lange [10], some interesting characteristics of the process emerge.

The slow crack growth process must, firstly, account for the vastly different propensities for slow crack growth in the sintered and hot-pressed materials. The different crystal structure (the hot-pressed material is hexagonal, whereas the sintered material is primarily cubic), is not likely to be an important factor; microstructural effects, especially second phases and impurities, are the most likely source of this slow crack growth disparity.

The primary second phase in the hot pressed material is the Al_2O_3 hot pressing additive which remains in the material after densification, as a residual grain-boundary phase [11]. The high temperature deformation characteristics of single crystal Al_2O_3 have been extensively studied (e.g. [12]). Within the temperature range 1200 to 1500° C, activation energies of 105 to 115 kcal mol^{-1} have been reported for different deformation phenomena [12], consistent with the values (120 to 130 kcal mol^{-1}) obtained for slow crack growth in the hot pressed SiC. This suggests that the deformation of the residual grain boundary located Al_2O_3 may account for the slow crack growth in this material.

The importance of certain impurities (especially CaO) has been demonstrated by adding small quantities of these impurities to the starting SiC + Al_2O_3 powders [10]. These impurities tend to segregate to the grain boundaries, possibly causing a glassy silicate to form [10]. At high temperatures, the viscous silicate allows grains to separate and slide causing cracks to slowly grow during stressing. Impurities such as CaO can lower the viscosity of the silicate, thereby enhancing the slow crack growth. Thus, the larger impurity content in the hot-pressed material (due to a different powder source) may also account for slow crack growth occurring in this material but not in the sintered material.

5. Conclusions

Fracture mechanics studies of a hot-pressed and a sintered silicon carbide have shown that slow crack growth occurs in both materials at room temperature in water, but only in the hot-pressed material at high temperatures (1000 to 1400° C). The slow crack growth mechanism at room temperature is probably stress corrosion, but the corrosion reaction has not been identified. The mechanism at high temperatures in the hot-pressed material is probably plastic flow controlled, due either to grain-boundary sliding or dislocation activity.

A good correlation of the observed fracture behaviour of flexural specimens, in both constant stress rate tests and in simulation proof tests (see Appendix 2) with the behaviour predicted from fracture mechanics parameters strongly suggests that the fracture mechanics data can be used for effective failure prediction in structural components made from this material.

Acknowledgements

Some of the experimental work was conducted while one of us (A. G. Evans) was located at the National Bureau of Standards. The work at N.B.S. was supported by the Aeronautics Research Laboratory, at the Westinghouse Research Laboratories by the Office of Naval Research (Contract No. N00014-68-C-0323), and at Rockwell under the Rockwell Independent Research and Development program.

Appendix 1. Activation energy determination from cyclic temperature tests

By assuming the following functional slow crack growth relation [5],

$$V = \alpha K^n \exp(-Q/RT) \qquad \text{(A1)}$$

where α and n are temperature independent constants, the apparent activation energy, Q, can

be determined from fracture mechanics or strength tests.

The most effective approach for obtaining Q from fracture mechanics tests utilizes a differential temperature technique, whereby the crack velocity is measured alternately at two different temperatures, T_1 and T_2, at constant K. Then we obtain from Equation A1,

$$\frac{\bar{V}_1}{\bar{V}_2} = \exp\left[\frac{Q}{R}\left(\frac{1}{T_2} - \frac{1}{T_1}\right)\right]_K \quad \text{(A2)}$$

where $\bar{V}_1$ and $\bar{V}_2$ are respectively the average crack velocities at T_1 and T_2. Rearranging then gives;

$$Q = \frac{RT_2T_1}{(T_2 - T_1)} \ln\left(\frac{V_2}{V_1}\right)_K. \quad \text{(A3)}$$

To obtain the activation energy from strength tests the median strengths measured at two different temperatures, and at a constant stress rate, can be used. Thus, substituting for K ($= \sigma Y\sqrt{a}$, where a is the crack length) in Equation A1 and putting $V = \mathrm{d}a/\mathrm{d}t$, we obtain;

$$\frac{\mathrm{d}a}{a^{n/2}} = \frac{\alpha Y^n}{\dot{\sigma}} \exp\left(\frac{-Q}{RT}\right) \sigma^n \, \mathrm{d}\sigma. \quad \text{(A4)}$$

Integrating Equation A4 to obtain the fracture stress gives;

$$\sigma_f^{n+1} = \frac{2\dot{\sigma}(n+1)}{\alpha Y^2 (n-2)} a_0^{n-2} \exp\left(\frac{Q}{RT}\right). \quad \text{(A5)}$$

Hence for two statistically compatible strength values of σ_{f1} and σ_{f2} obtained at the same stress rate at temperatures T_1 and T_2, we obtain from Equation A5,

$$\left(\frac{\sigma_{f1}}{\sigma_{f2}}\right)_{\dot{\sigma}}^{n+1} = \exp\left[\frac{Q}{R}\left(\frac{1}{T_1} - \frac{1}{T_2}\right)\right]. \quad \text{(A6)}$$

Then, rearranging gives;

$$Q = \frac{RT_1T_2}{T_2 - T_1}(n+1)\left|\ln\left(\frac{\sigma_{f1}}{\sigma_{f2}}\right)\right|_{\dot{\sigma}}. \quad \text{(A7)}$$

Appendix 2. Stress/time/temperature cycling for hot-pressed SiC

A critical demonstration of the utility of fracture mechanics data for predicting failure in silicon carbide can be provided by subjecting test specimens to a stress/time/temperature cycle and comparing the predicted crack growth with failure measurements. A cycle which might have some practical importance, e.g. when devising a proof test procedure [13] for components made from this material, is shown schematically in Fig. 5. The first loading was performed at 800° C using a stress rate of $17\,\mathrm{MN\,m^{-2}\,sec^{-1}}$, to $650\,\mathrm{MN\,m^{-2}}$; then, if fracture did not occur, the stress was held for ~ 1 min and then reduced very rapidly (in ~ 0.1 sec) to $7\,\mathrm{MN\,m^{-2}}$. The temperature was then

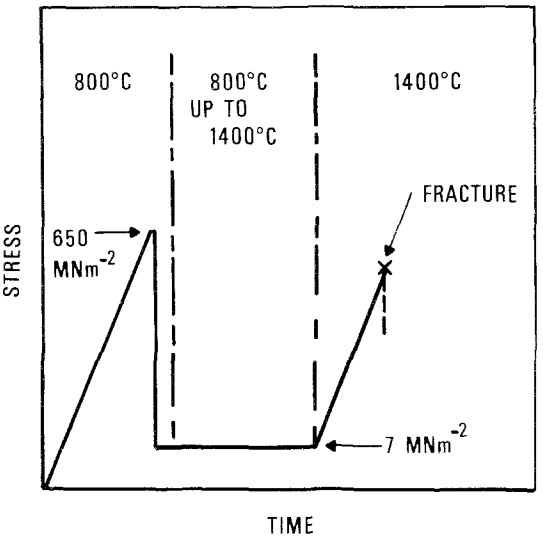

Figure 5 A schematic of the stress/time/temperature cycle used for the test series described in the test.

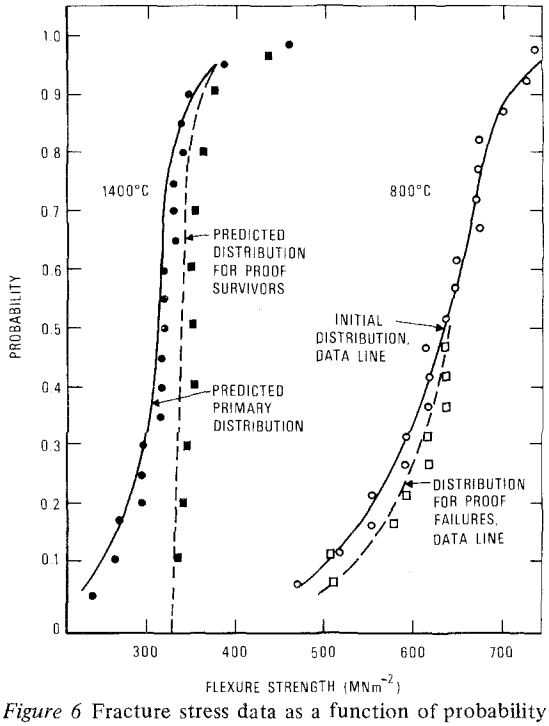

Figure 6 Fracture stress data as a function of probability at 800 and 1400° C for constant stress rate tests and for the test cycle shown in Fig. 5. Also shown are the strengths at 1400° C predicted from the 800° C data and the fracture mechanics data (Fig. 2).

increased to 1400° C at constant stress (maintained using a load cycling attachment) and finally, the stress was increased at 17 $MN\,m^{-2}\,sec^{-1}$ until fracture occurred.

The fracture stress data obtained using this test procedure, compared to the constant stress rate fracture stress data at 800 and 1400° C, are shown in Fig. 6. It is apparent that the fracture of approximately half the specimens at 800° C has truncated the 1400° C fracture stress distribution for the survivors, in qualitative accord with the expectations for a flaw propagation controlled failure process. A more quantitative crack growth analysis can also be performed, using Equation 2, as indicated by the predicted lines in Fig. 6. The good comparison with the measured fracture stress data amply confirms the validity of crack growth predictions from fracture mechanics data, and also suggests that proof testing may be a viable procedure for this material.

References

1. F. F. LANGE, ASME pub. 72-GT-56.
2. S. M. WIEDERHORN, "Fracture Mechanics of Cermaics", edited by R. C. Bradt, D. P. H. Hasselman and F. F. Lange (Plenum, New York, 1974) p. 613.
3. D. P. WILLIAMS and A. G. EVANS, *J. Testing and Evaluation* **1**, (1973 264.
4. S. M. WIEDERHORN, A. M. SHORB and R. L. MOSES, *J. Appl. Phys.* **39** (1968) 1572.
5. A. G. EVANS, L. R. RUSSELL and D. W. RICHERSON, *Met. Trans.* **6A** (1975) 707.
6. F. F. LANGE, *J. Amer. Ceram. Soc.* **57** (1974) 84.
7. S. M. WIEDERHORN and L. H. BOLTZ, *ibid* **53** (1970) 543.
8. A. G. EVANS, *Int. J. Fract.* **10** (1974) 251.
9. *Idem.* "Ceramics for High Performance Applications", AMMRC Pub., p. 373.
10. F. F. LANGE, *ibid*, p. 223.
11. F. F. LANGE, *J. Mater. Sci.*, **10** (1975) 314.
12. H. CONRAD, G. STONE and K. JANOWSKI, *Trans. Met. Soc. AIME* **233** (1965) 889.
13. A. G. EVANS and S. M. WIEDERHORN, *Intl. J. Fract.* **10** (1974) 379.

Received 3 March 1975 and accepted 26 March 1975.